Cell Reports, Volume *36*

Supplemental information

Cell-autonomous inflammation of *BRCA1*-deficient ovarian cancers drives both tumor-intrinsic immunoreactivity and immune resistance *via* STING

Marine Bruand, David Barras, Marco Mina, Eleonora Ghisoni, Matteo Morotti, Evripidis Lanitis, Noémie Fahr, Mathieu Desbuisson, Alizée Grimm, Hualing Zhang, Chloe Chong, Julien Dagher, Sora Chee, Theodora Tsianou, Julien Dorier, Brian J. Stevenson, Christian Iseli, Catherine Ronet, Sara Bobisse, Raphael Genolet, Josephine Walton, Michal Bassani-Sternberg, Lana E. Kandalaft, Bing Ren, Iain McNeish, Elizabeth Swisher, Alexandre Harari, Mauro Delorenzi, Giovanni Ciriello, Melita Irving, Sylvie Rusakiewicz, Periklis G. Foukas, Fabio Martinon, Denarda Dangaj Laniti, and George Coukos

Supplementary Figure S1

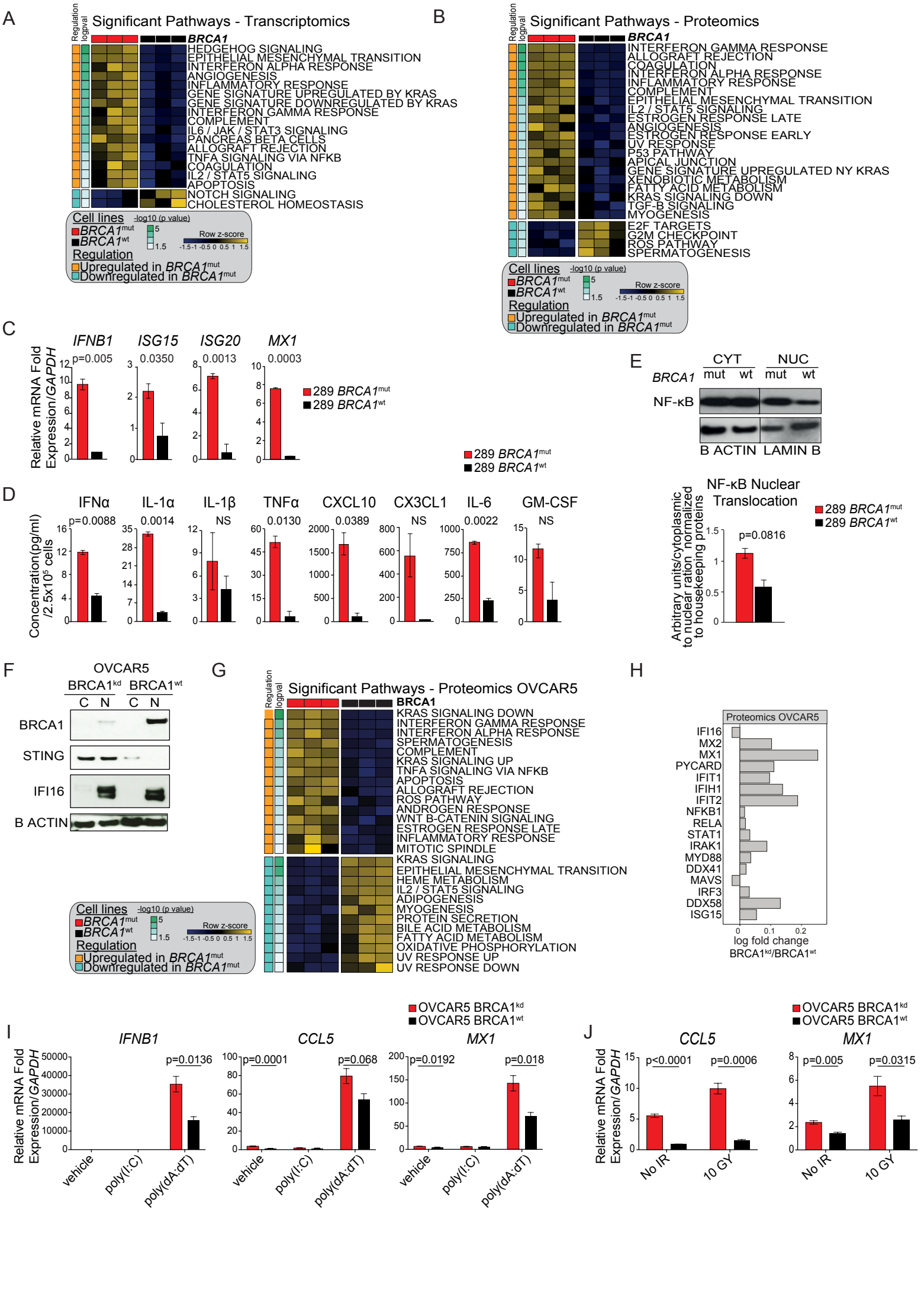

Supplementary Figure S1 (related to Figure 1)

***BRCA1* loss leads to increased cell-autonomous inflammatory activation in ovarian cancer cells**

A. Heatmap of Hallmarks signatures with significantly different enrichment score between *BRCA1*^{mut} and *BRCA1*^{wt} isogenic cell lines (<adjusted p value of 0.05 after linear regression) at the transcriptomics level.

B. Heatmap of Hallmarks signatures with significantly different enrichment score between *BRCA1*^{mut} and *BRCA1*^{wt} isogenic cell lines (<adjusted p value of 0.05 after linear regression) at the proteomics level.

C. Real-time (RT)-PCR analysis of *IFNB1*, *ISG15*, *ISG20* and *MX1* in *BRCA1*^{mut} and *BRCA1*^{wt} isogenic cell lines (mean ± SEM; n=3). P values were calculated with unpaired T test.

D. Cytokine Bead Array (CBA) analysis of IFNα, IL-1α, IL-1β, TNF, CXCL10, CX3CL1, IL-6 and GM-CSF in cell-free supernatants of *BRCA1*^{mut} and *BRCA1*^{wt} cells isogenic cell lines. The concentration (pg/ml) was normalized to cell number ($2.5x10^5$) (mean± SEM; n=2). P values were calculated with unpaired T test.

E. Western blot analysis (up) and summary quantification (down) of NF-κB (p65) detection in the cytoplasmic (CYT) and nuclear (NUC) fractions of *BRCA1*^{mut} and *BRCA1*^{wt} isogenic cell lines (mean ± SEM; n=2).

F. Western blot analysis of cytoplasmic (C) and nuclear (N) fractions of OVCAR5 BRCA1^{kd} and BRCA1^{wt} isogenic cell lines for BRCA1, STING, IFI16 and B ACTIN as a loading control.

G. Heatmap of Hallmarks signatures with significantly different enrichment score between OVCAR5 BRCA1 isogenic cell lines (<adjusted p value of 0.05 after linear regression) at the proteomics level.

H. Protein levels of the nucleic acid sensing and IFN activation pathway between the OVCAR5 BRCA1 isogenic cell lines as quantified by Mass spectrometry proteomics.

I. RT-PCR analysis of *IFNB1*, *CCL5* and *MX1* expression of OVCAR5 BRCA1^{kd} and BRCA1^{wt} isogenic cell lines 6-hour post stimulation with liposomes or liposomes loaded with poly(I:C) or poly(dA:dT) (mean ± SEM; n=3). P values were calculated with unpaired T test.

J. RT-PCR analysis of *CCL5* and *MX1* in OVCAR5 BRCA1^{kd} and BRCA1^{wt} isogenic cell lines 48 hours post irradiation (mean ± SEM; n=3). P values were calculated with unpaired T test.

Supplementary Figure S2

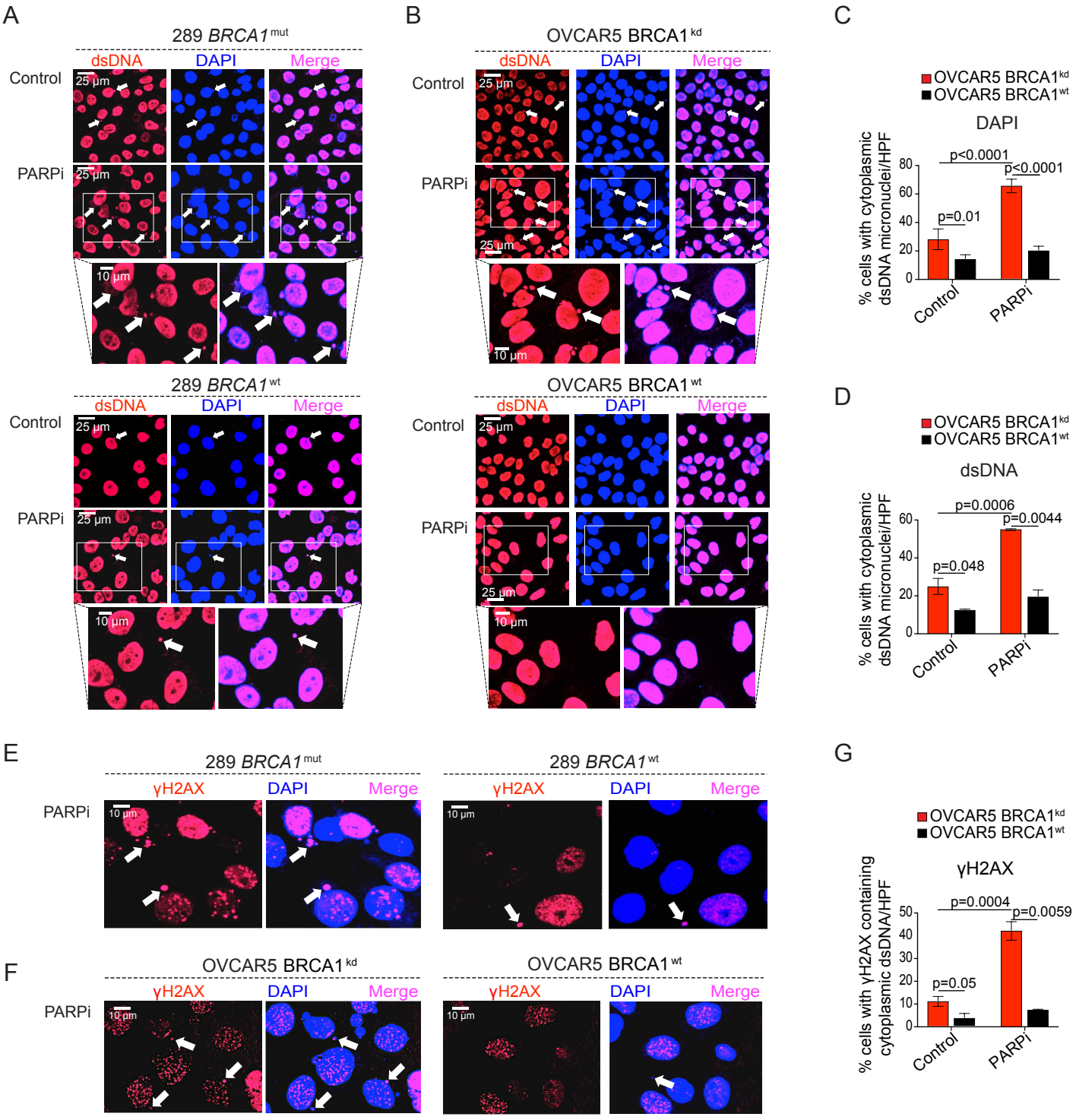

Supplementary Figure S2 (related to Figure 2)

***BRCA1*-silenced cells accumulate cytoplasmic dsDNA, which is exacerbated by PARP inhibition**

A.B. Confocal microscopy analysis of cytoplasmic dsDNA micronuclei in UWB1.289 *BRCA1*^{mut} and *BRCA1*^{wt} (A) and OVCAR5 BRCA1^{kd} and BRCA1^{wt} (B) isogenic cell lines detected by an anti-dsDNA Ab (red) or DAPI (blue) 48 hours post treatment with DMSO or olaparib (10 μg/ml). Cytoplasmic DNA was co-stained by DAPI. Examples of cytoplasmic dsDNA micronuclei are indicated by white arrows. Scale bar 25 μm.

C.D. Summary quantification of the percentage of cells/high power field (HPF) carrying cytoplasmic dsDNA micronuclei as detected by DAPI (C) and anti-dsDNA-specific antibody (D) in OVCAR5 BRCA1^{kd} and BRCA1^{wt} isogenic cell lines treated with DMSO or olaparib (mean ± SEM; n= 4). P values were calculated with unpaired T test.

E.F. Confocal microscopy analysis of histone-derived cytoplasmic dsDNA micronuclei as detected by anti-γH2AX (red) and DAPI (blue) in UWB1.289 (E) and OVCAR5 (F) BRCA1 isogenic cell lines 48 hours post treatment with DMSO or olaparib. Examples of cytoplasmic dsDNA micronuclei are indicated by white arrows. Scale bar 10 μm.

G. Summary quantification of the percentage of cells/HPF carrying histone-derived cytoplasmic dsDNA as detected by anti-γH2AX in OVCAR5 BRCA1^{kd} and BRCA1^{wt} isogenic cell lines treated with DMSO or olaparib (mean ± SEM; n= 3). P values were calculated with unpaired T test.

Supplementary Figure S3

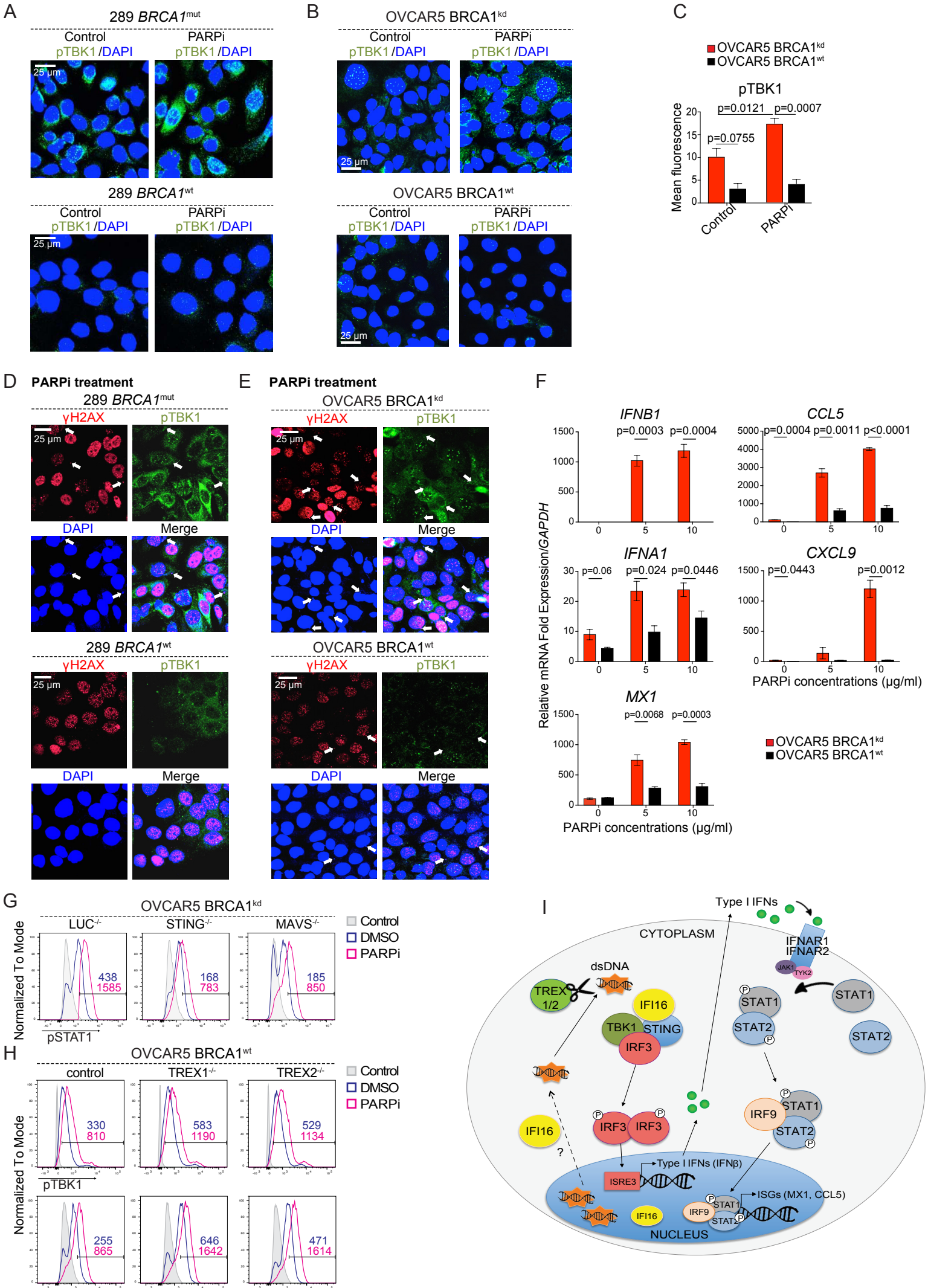

Supplementary Figure S3 (related to Figure 2)

***BRCA1* loss in ovarian cancer cells leads to cell-autonomous inflammatory state through tumor cell intrinsic STING/pTBK1 pathway activation**

A.B. Confocal microscopy analysis of phosphorylated TBK1 (green) and DAPI (blue) in UWB1.289 (A) and OVCAR5 (B) isogenic cell lines 48 hours post treatment with DMSO or olaparib. Scale bar 25 µm.

C. Quantification of the mean fluorescence intensity (MFI) of pTBK1 staining in OVCAR5 $BRCA1^{kd}$ and $BRCA1^{wt}$ treated with DMSO or olaparib (mean ± SEM; n=3). P values assessed by One-way ANOVA.

D.E. Confocal analysis of phosphorylated TBK1 (green), γH2AX (red) and DAPI (blue) in UWB1.289 (D) and OVCAR5 (E) BRCA1 isogenic cell line pair 48 hours post treatment with olaparib. White arrows show examples of cytoplasmic dsDNA micronuclei labelled by both DAPI and γH2AX and surrounded by phosphorylated TBK1. Scale bar 25 µm.

F. RT-PCR analysis of *IFNB1*, *IFNA1*, *MX1*, *CCL5* and *CXCL9* expression in OVCAR5 $BRCA1^{kd}$ and $BRCA1^{wt}$ cell lines 48 hours post treatment with olaparib (mean ± SEM; n=3). P values assessed by unpaired T test.

G. Representative histograms of intracellular pSTAT1 expression in OVCAR5 $BRCA1^{kd}$ cells crispered for Luciferase, IFI16, STING and MAVS 48 hours post treatment with DMSO or olaparib. Indicated numbers represent pSTAT1 MFI in the control (blue) and PARPi (pink) conditions.

H. Representative histograms of intracellular pTBK1 and pSTAT1 expression in OVCAR5 $BRCA1^{kd}$ cells transduced with a control, TREX1 or TREX2 CRISPR-Cas9 lentiviral vector 48 hours post treatment with DMSO or olaparib. Indicated numbers represent pSTAT1 MFI in the control (blue) and PARPi (pink) conditions.

I. Cartoon illustration of the molecular cascade which leads to sensing of histone-derived dsDNA by the IFI16/STING/TBK1 complex and then subsequent activation of the type I IFN pathway through IRF3 phosphorylation in *BRCA1*-deficient cells. TREX1/2 regulate this activation by degrading cytosolic dsDNA. Type I IFNs can maintain an inflamed cell phenotype through autocrine STAT1 signaling and transcription of IFN induced genes (*i.e. MX1*) and chemokines (*CCL5*, *CXCL9*, *CXCL10*, etc).

Supplementary Figure S4

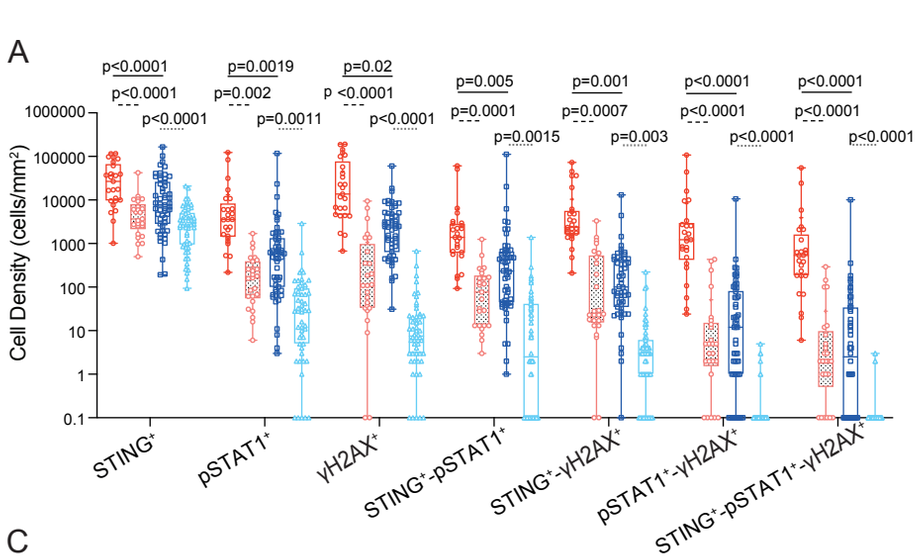

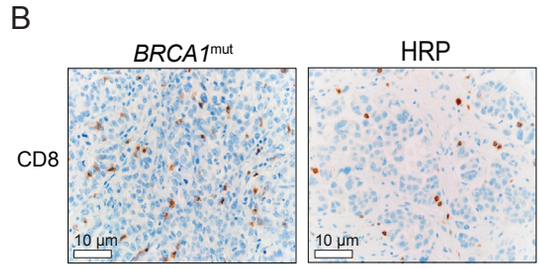

C

	Tumor cells (CK +)						
Correlations of i.e. CD8 with:	STING+	pSTAT1+	γH2AX+	STING+-γH2AX+	STING+-pSTAT1+	pSTAT1+-γH2AX+	STING+-pSTAT1+-γH2AX+
r (Pearson's) in *BRCA1*mut and HRP HGSOC	0.420821562	0.153969697	0.0806591	0.099173671	0.109463542	0.137652766	0.143302046
p value in *BRCA1*mut and HRP HGSOC	0.000113	0.175681	0.480114	0.38489	0.337179	0.337179	0.207709
r (Pearson's) in *BRCA1*mut HGSOC	0.450153716	0.43129939	0.13077899	0.157081352	0.478056779	0.262015917	0.285768179
p value in *BRCA1*mut HGSOC	0.023966	0.031391	0.533466	0.453569	0.01566	0.205809	0.166229
	Stromal cells (CK -)						
Correlations of i.e. CD8 with:	STING+	pSTAT1+	γH2AX+	STING+-γH2AX	STING+-pSTAT1+	pSTAT1+-γH2AX+	STING+-pSTAT1+-γH2AX+
r (Pearson's) in *BRCA1*mut and HRP HGSOC	0.164318074	0.137315157	0.05941612	0.21049522	-0.001675694	0.210993748	0.115156632
p value in *BRCA1*mut and HRP HGSOC	0.147923	0.227578	0.603061	0.062721	0.993021	0.062085	0.312454
r (Pearson's) in *BRCA1*mut HGSOC	0.204167112	0.52064315	0.08122008	0.413191015	-0.066377372	0.653527099	0.203124939
p value in *BRCA1*mut HGSOC	0.327774	0.007629	0.699606	0.040125	0.753941	0.000397	0.330201

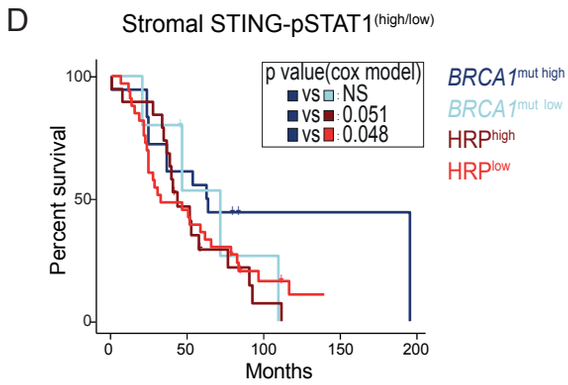

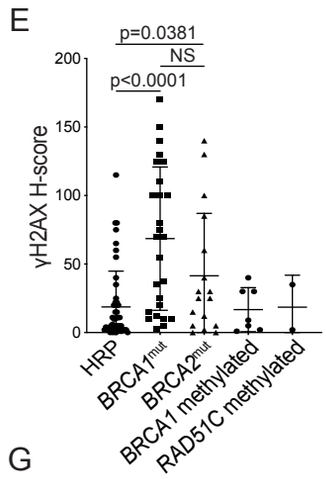

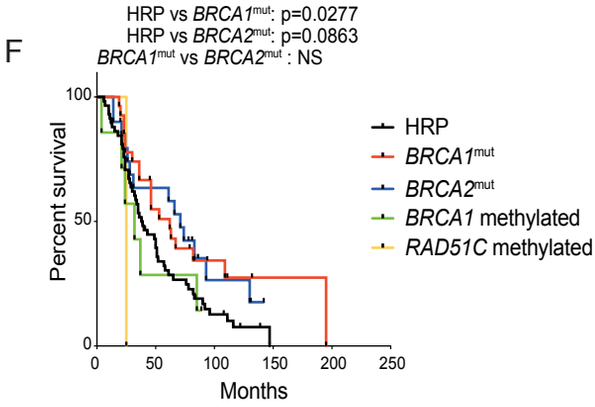

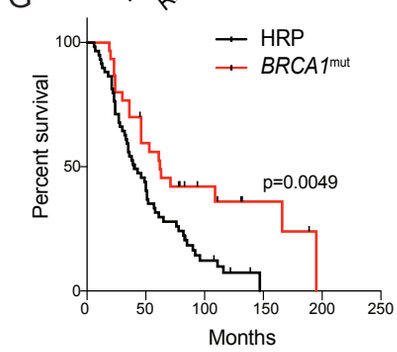

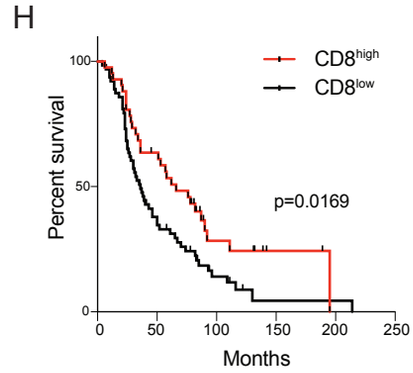

Supplementary Figure S4 (related to Figures 3 and 4)

***BRCA1* deficiency associates with CD8$^+$ T cell inflammation, dsDNA sensing, IFN activation and better overall survival**

A. Quantification of γH2AX$^+$, STING$^+$ and/or pSTAT1$^+$ tumor (CK$^+$) and stromal (CK$^-$) cells in BRCA1^{mut} (n=25) and HR proficient (HRP) (n=54) HGSOC. Boxplots represent 25th and 75th percentiles with the midline indicating the median; whiskers extend to the lowest/highest values and points indicate values for individual subjects. P values were calculated with Mann-Whitney test.

B. Representative immunohistochemical staining of intraepithelial (i.e.) CD8$^+$ T cell infiltration in BRCA1^{mut} and HRP HGSOC. Scale bar 10 µm.

C. Pearson's correlations and p values of i.e. TIL with tumor tumor (CK$^+$) and stromal (CK$^-$) cells expressing pSTAT1$^+$ or STING$^+$ or γH2AX in patients with *BRCA1*^{mut} or *BRCA1/2*^{wt} carcinomas.

D. Kaplan-Mayer survival analysis of *BRCA1*^{mut} and HRP HGSOC expressing high or low levels of stromal STING and pSTAT1. P values were extracted from Cox proportional-hazards tests.

E. Quantification of γH2AX in HRP, *BRCA1*- or *BRCA2*-deficient (*BRCA1/2*^{mut}) and *BRCA1* or *RAD51C* methylated HGSOC tumors (mean ± SEM). Points indicate values for individual subjects. P values were calculated with Mann-Whitney test.

F. Kaplan-Mayer survival analysis of patients with HRP (n=58), *BRCA1*^{mut} (n=27), *BRCA2*^{mut} (n=20), *BRCA1* (n=7) or *RAD51C* (n=2) methylated HGSOC. P values were extracted from Cox proportional-hazards tests.

G. Kaplan-Mayer survival analysis of patients with *BRCA1*^{mut} (n=30) and HRP (n=59) HGSOC. P values were extracted from Cox proportional-hazards tests.

H. Kaplan-Mayer survival analysis of patients with CD8^{high} (n=42) and CD8^{low} (n=63) i.e. T cell infiltration in HGSOC (mean ± SEM). P values were extracted from Cox proportional-hazards tests.

Supplementary Figure S5

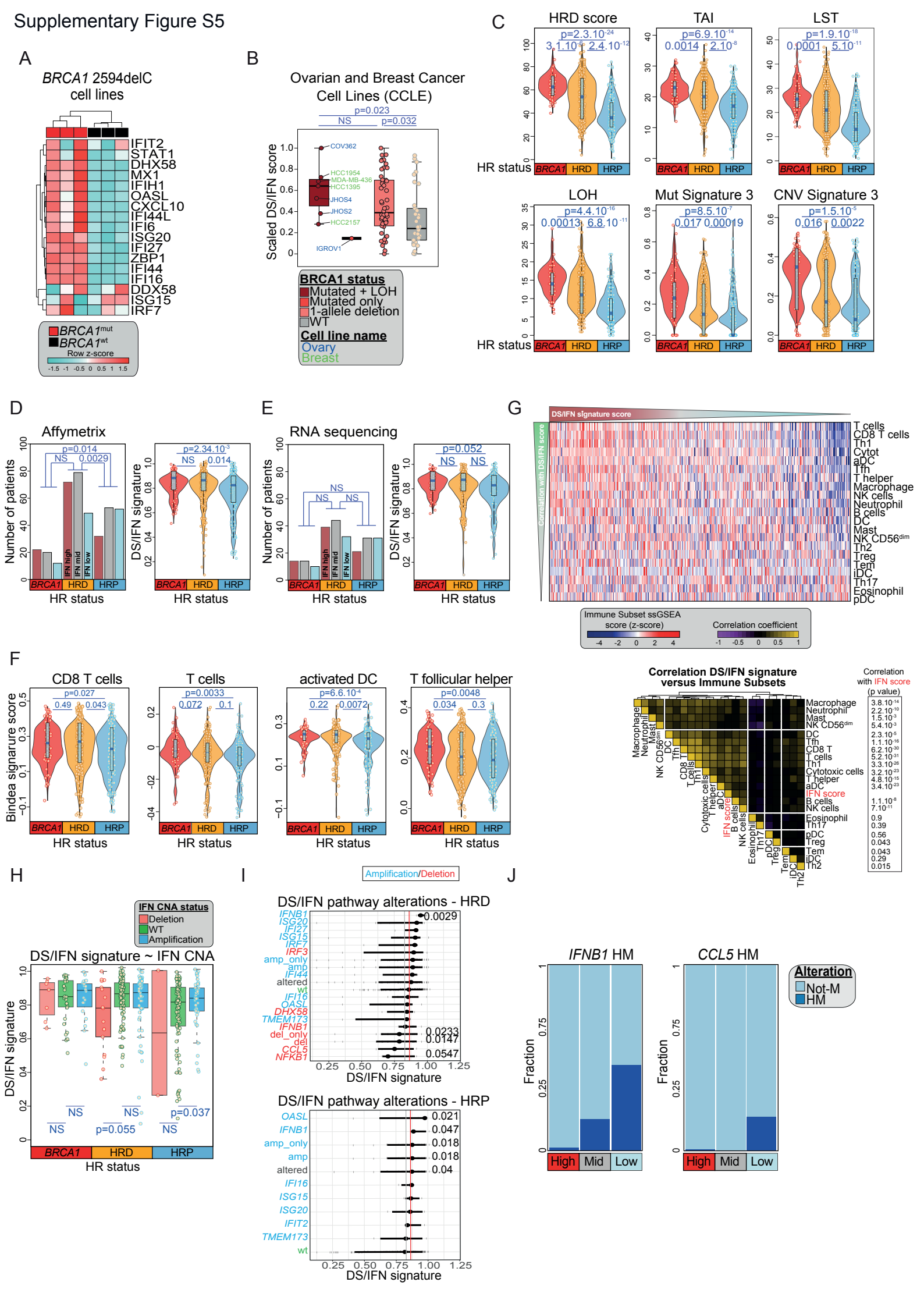

Supplementary Figure S5 (related to Figure 5)

Association between homologous recombination, DS/IFN pathway and immune landscape of HGSOC.

A. Heat map showing hierarchal clustering of DNA sensing/interferon-related gene expression in *BRCA1*^{wt} and *BRCA1*^{mut} isogenic cell lines.

B. Comparison of the DS/IFN score in ovarian and breast cancer lines from the Cancer Cell Line Encyclopedia (CCLE) carrying *BRCA1* mutations and LOH (complete *BRCA1* functional loss), CNV only (1 allele deletion) and *BRCA1*^{wt} lines. Boxplots represent 25th and 75th percentiles with the midline indicating the median; whiskers extend to the lowest/highest values and points indicate values for individual cell lines. Statistical significance assessed by Wilcoxon rank-sum tests.

C. Association between *BRCA1,* HR deficient (HRD) and proficient (HRP) HGSOC and HRD score, telomere allelic imbalance (TAI), large-scale state transition (LST) (Gonzalez-Martin et al.), LOH and mutational and CNV signatures 3. Violin plots extend to lowest/highest values and points indicate values for individual subjects. Median is displayed by middle lines. Statistical significance assessed by Wilcoxon rank-sum tests.

D. E. Left bar graphs: Comparison of the number of *BRCA1*^{mut}, HRD and HRP HGSOC that express high, medium and low DS/IFN signature scores, respectively, in Affymetrix (D) and RNA-sequencing (E) platforms of the TCGA. Statistical significance computed by Fisher's Exact test comparing high and low IFN groups according to HRD groups. Right Violin plots: Comparison of the DS/IFN score between *BRCA1*^{mut}, HRD and HRP HGSOC in Affymetrix (D) and RNA-sequencing (E) platforms of the TCGA. Points indicate values for individual subjects. Statistical significance assessed by Wilcoxon rank-sum tests.

F. Comparison of the Bindea CD8 T cell, T cells, activated DC and T follicular helper signature scores (Bindea et al., 2013) in *BRCA1*^{mut}, HRD and HRP HGSOC. Points indicate values for individual subjects. Statistical significance assessed by Wilcoxon rank-sum tests.

G. Correlation heatmap displaying R coefficients between immune subset scores and the DS/IFN score. P values of correlation tests between the DS/IFN signature and the immune subsets are reported on the right.

H. Comparison of the DS/IFN score in *BRCA1*^{mut}, HRD and HRP HGSOC according to DS/IFN genes copy number alteration status (Agilent platform). Points indicate values for individual subjects. Statistical significance assessed by Wilcoxon rank-sum tests.

I. Association between DS/IFN-related gene impairment (deletion/amplification) in y axis and interferon pathway activation (DS/IFN signature score expression) in x axis, in HRD (up) and HRP (down) TCGA human ovarian cancers in Agilent. IFN pathway genomic alteration status was evaluated as described in the methods. Whiskers represent 25th and 75th percentiles with middle dots indicating the median. Each dot represents an individual tumor. Significant p values are shown in the graphs.

J. Fraction plot showing the abundance of hypermethylation (HM) events of *IFNB1* or *CCL5* in the IFN groups in TCGA HGSOC.

Supplementary Figure S6

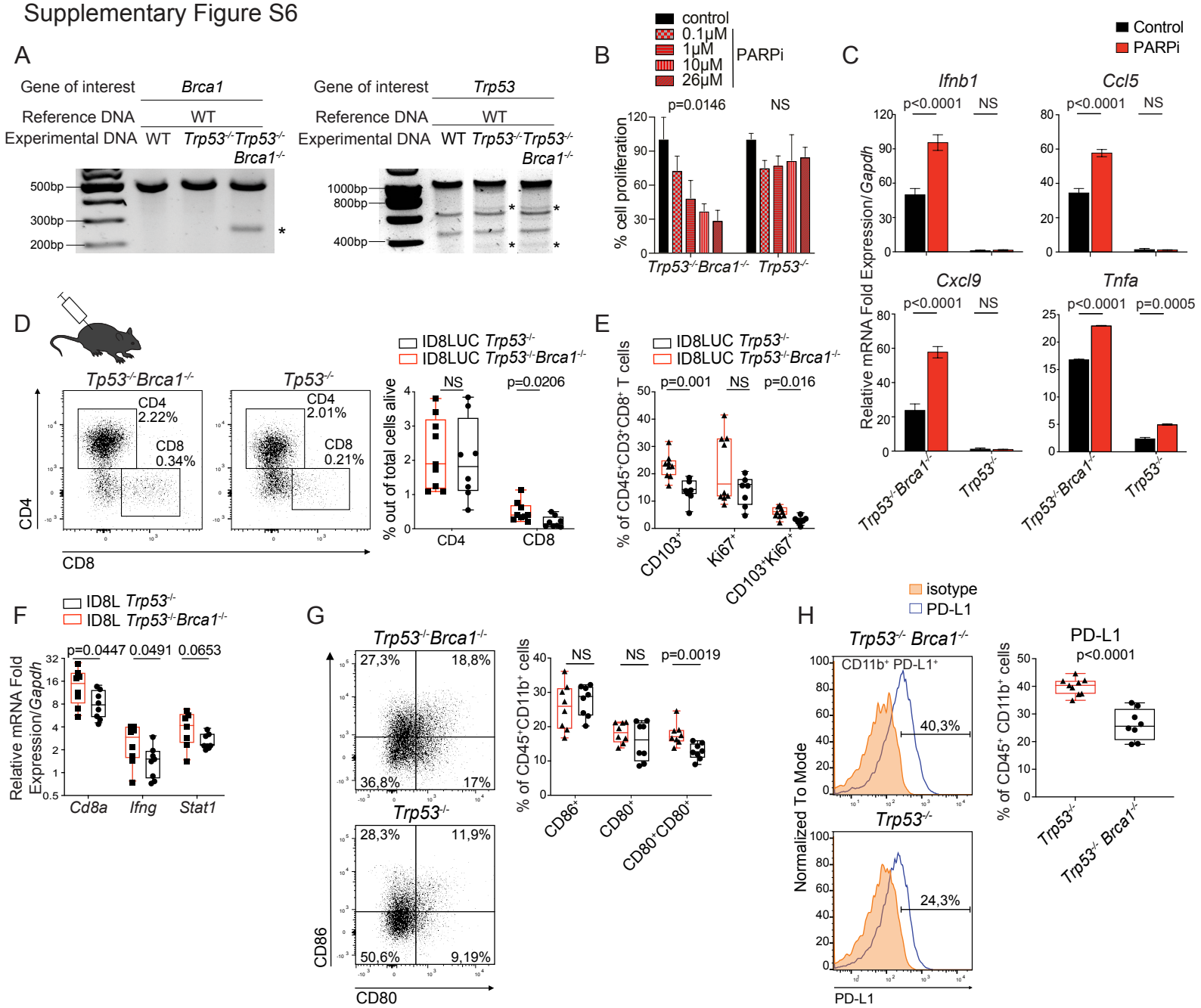

Supplementary Figure S6 (related to Figure 5)

Mouse ovarian *Brca1*-deficient cancers are immunogenic *in vivo*

A. Surveyor assay for the detection of CRISPR-CAS9 induced mutations in the *Trp53* and *Brca1* genes of the ID8 *Trp53*$^{-/-}$*Brca1*$^{-/-}$ and *Trp53*$^{-/-}$*Brca1*^{wt} cell lines. Asterisks indicate DNA bands that are different from WT and occur in the cell lines of interest.

B. MTT proliferation assay showing the sensitivity of ID8Luc *Trp53*$^{-/-}$*Brca1*$^{-/-}$ and *Trp53*$^{-/-}$*Brca1*^{wt} isogenic cell lines to PARP inhibition 24 hours post treatment with the indicated concentrations (mean ± SEM; n=2).

C. RT-PCR analysis of *Ifnb1*, *Ccl5*, *Cxcl9* and *Tnfa* expression in ID8Luc *Trp53*$^{-/-}$*Brca1*$^{-/-}$ and *Trp53*$^{-/-}$*Brca1*^{wt} isogenic cell lines 48 hours post treatment with olaparib (mean ± SEM; n=3). P values were calculated with unpaired T test.

D. Representative FACS dot plots and quantification of CD4^{+} and CD8^{+} TILs in ID8Luc *Trp53*$^{-/-}$*Brca1*$^{-/-}$ (n=9) and *Trp53*$^{-/-}$*Brca1*^{wt} (n=8) i.p. syngeneic tumors. Boxplots represent 25th and 75th percentiles with the midline indicating the median; whiskers extend to the lowest/highest values. Points indicate values for individual subjects. P values were calculated with Mann-Whitney test.

E. *Ex vivo* FACS analysis and comparison of CD103 and Ki67 expression in CD8^{+} T cells in ID8Luc *Trp53*$^{-/-}$*Brca1*$^{-/-}$ (n=9) and *Trp53*$^{-/-}$*Brca1*^{wt} (n=8) i.p. syngeneic tumors. Boxplots represent 25th and 75th percentiles with the midline indicating the median; whiskers extend to the lowest/highest values. Points indicate values for individual subjects. P values were calculated with Mann-Whitney test.

F. RT-PCR analysis of *Cd8a*, *Ifng* and *Stat1* expression in ID8Luc *Trp53*$^{-/-}$*Brca1*$^{-/-}$ (n=9) and *Trp53*$^{-/-}$*Brca1*^{wt} (n=8) i.p syngeneic tumors. Boxplots represent 25th and 75th percentiles with the midline indicating the median; whiskers extend to the lowest/highest values. Points indicate values for individual subjects. P values were calculated with unpaired T test.

G. Representative FACS dot plots and quantification of CD80 and CD86 expression in CD11b^{+} cells in ID8Luc *Trp53*$^{-/-}$*Brca1*$^{-/-}$ (n=9) and *Trp53*$^{-/-}$*Brca1*^{wt} (n=8) i.p syngeneic tumors. Boxplots represent 25th and 75th percentiles with the midline indicating the median; whiskers extend to the lowest/highest values. Points indicate values for individual subjects. P values were calculated with Mann-Whitney test.

H. Representative histograms and *ex vivo* FACS quantification of surface PD-L1 expression in CD11b^{+} cells in ID8Luc *Trp53*$^{-/-}$*Brca1*$^{-/-}$ (n=9) and *Trp53*$^{-/-}$*Brca1*^{wt} (n=8) i.p. syngeneic tumors. P values were calculated with Mann-Whitney test.

Supplementary Figure S7

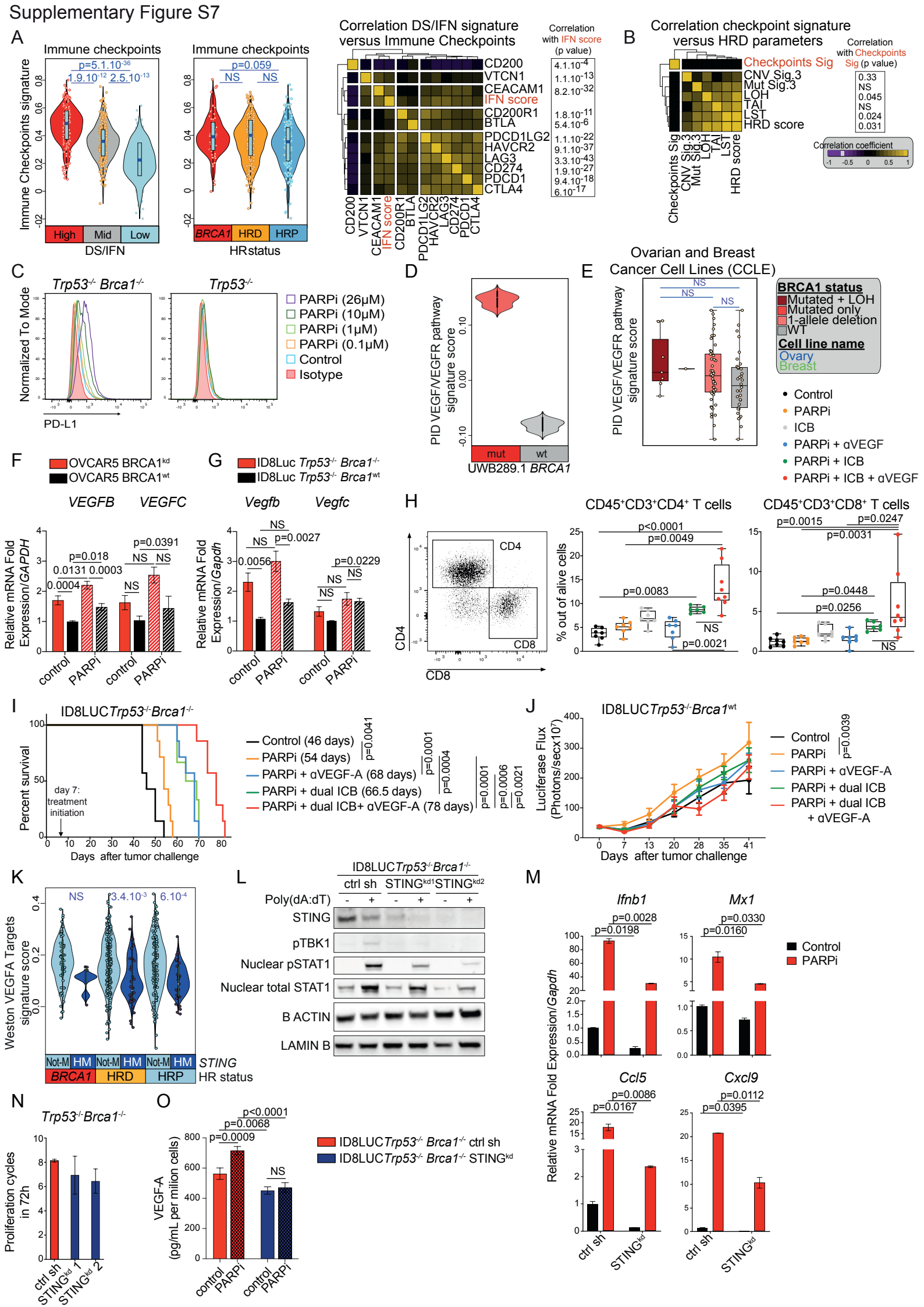

Supplementary Figure S7 (related to Figure 7)

Tumor-intrinsic STING promotes resistance to dual immunotherapy *via* VEGF-A

A. Left: Association between DS/IFN and immune checkpoint signatures in the TCGA HGSOC cohort. Middle: Association between immune checkpoint signature score and HRD groups. Points indicate values for individual subjects. Violin plots extend to lowest/highest values and embedded vertical boxes represent the 25th and 75th percentiles. Median is displayed by middle lines. Statistical significance assessed by Wilcoxon rank-sum tests. Right: Correlation heatmap displaying Pearson's R coefficients between expression of the immune checkpoint genes and the DS/IFN signature score. Violin plots extend to lowest/highest values and embedded vertical boxes represent the 25th and 75th percentiles. Median is displayed by middle lines. P values of correlation tests are reported for the indicated comparisons.

B. Correlation heatmap between the immune checkpoint signature and genomic HRD signatures. P values of correlation tests are reported for the indicated comparisons.

C. FACS analysis of surface PD-L1 expression in ID8 *Trp53*$^{-/-}$*Brca1*$^{-/-}$ and *Trp53*$^{-/-}$*Brca1*^{wt} isogenic cell lines 48 hours post olaparib treatment at the indicated concentrations.

D. Comparison of the PID VEGF/VEGFR pathway signature score (Schaefer et al., 2009) between UWB1.289 *BRCA1*^{mut} and *BRCA1*^{wt} cell lines (n=3). Violin plots extend to lowest/highest values and embedded vertical boxes represent the 25th and 75th percentiles. Median is displayed by middle lines.

E. Comparison of the PID VEGF/VEGFR pathway signature score (Schaefer et al., 2009) in ovarian and breast cancer lines from the Cancer Cell Line Encyclopedia (E) carrying *BRCA1* mutations and LOH (complete *BRCA1* functional loss), *BRCA1* mutation only, CNV only (1-allele deletion) or no alteration in *BRCA1* (WT). Boxplots represent 25th and 75th percentiles with the midline indicating the median; whiskers extend to the lowest/highest values. Points indicate values for individual subjects. Statistical significance assessed by Wilcoxon rank-sum tests.

F.G. Real-time PCR analysis of *VEGFB* and *VEGFC* expression in OVCAR5 BRCA1^{kd} and BRCA1^{wt} (n=8) (F) and ID8Luc *Trp53*$^{-/-}$*Brca1*$^{-/-}$ and ID8Luc *Trp53*$^{-/-}$*Brca1*^{wt} (n=4) (G) 48 hours post treatment with olaparib. Data are presented as mean ± SEM. P values were calculated with One-way ANOVA.

H. Representative FACS dot plots and quantification of CD4^{+} and CD8^{+} TILs in ID8Luc *Trp53*$^{-/-}$*Brca1*$^{-/-}$ i.p. tumors treated with control, olaparib, αCTLA-4+αPD-L1, αVEGFA or their combinations (n=6-8 per group). All boxplots represent 25th and 75th percentiles with the midline indicating the median; whiskers extend to the lowest/highest values. Points indicate values for individual subjects. P values were calculated with Mann-Whitney test.

I. Kaplan-Meier curves showing survival of mice with i.p. ID8Luc *Trp53*$^{-/-}$*Brca1*$^{-/-}$ cancers treated with indicated regimen (n=7-8 per group). P values were calculated with a log rank (Mantel-Cox) test.

J. I.p. tumor growth kinetics of ID8Luc *Trp53*$^{-/-}$*Brca1*^{wt} cancers during treatment with control, PARPi, dual ICB, αVEGFA or their combinations (n=6-7 per group). Data are presented as mean± SEM. P values assessed by Two-way ANOVA.

K. Comparison of the Weston VEGF targets signature score between *BRCA1*, HRD or HRP TCGA HGSOC with (HM) or without *STING* hypermethylation (Not-M). Violin plots extend to lowest/highest values and points indicate values for individual subjects. Median is displayed by middle lines. Statistical significance assessed by Wilcoxon rank-sum tests.

L. Western Blot analysis of STING, pTBK1, pSTAT1 and STAT1 in ID8Luc *Trp53*$^{-/-}$*Brca1*$^{-/-}$ STING^{kd} and scr sh treated with poly(dA:dT). The signal obtained for each protein was normalized to that of housekeeping proteins, B ACTIN and LAMIN B, in cytoplasmic and nuclear extracts, respectively.

M. Real-time PCR analysis of *Ifnb1*, *Mx1*, *Ccl5* and *Cxcl9* expression in ID8Luc *Trp53*$^{-/-}$*Brca1*$^{-/-}$ STING^{kd} and scr sh cell lines treated with DMSO or PARPi (mean± SEM; n=2). P values were calculated with unpaired T test.

N. Quantification of the number of proliferation cycles ID8Luc *Trp53*$^{-/-}$*Brca1*$^{-/-}$ STING^{kd} and scr sh cell lines achieved in 72h (mean± SEM; n=2).

O. ELISA analysis of mouse VEGF-A in cell-free supernatants of ID8Luc *Trp53*$^{-/-}$*Brca1*$^{-/-}$ STING^{kd} and scr sh cell lines. The concentration (pg/ml) was normalized to cell number (mean± SEM; n=3). P values were calculated with One-way ANOVA.